11th Australasian Fluid Mechanics Conference
University of Tasmania, Hobart, Australia
14-18 December 1992

POLLUTANT DISPERSION IN CHANNELS OF COMPLEX CROSS-SECTION

R.I. NOKES[1] and G.O. HUGHES[2]

[1]Dept of Engineering Science, University of Auckland, Auckland, NEW ZEALAND

[2]Dept of Applied Mathematics & Theoretical Physics, University of Cambridge, Cambridge, UNITED KINGDOM

ABSTRACT

A new semi-analytic method, based on a two-dimensional eigenfunction solution, for solving steady, turbulent mixing problems in uniform channels of irregular cross-section, is presented The implementation of the method is discussed, and results are compared with the experimental results of Wood and Liang (1989).

1 INTRODUCTION

Turbulent dispersion in rectangular channels has received considerable attention in the literature. Studies have focussed on longitudinal, vertical and lateral dispersion and our understanding of the important physical processes is well advanced, although some uncertainty about the numerical values of parameters such as the lateral turbulent diffusivity still remain.

Attention is now turning to the rather more difficult, but also more practical, problems of the flow and mixing characteristics of channels whose cross-section is irregular. An example is a river comprising a main channel and a flood plain. Knight and his co-workers (see Shiono and Knight, 1991) have performed extensive laboratory experiments aimed at measuring mean and turbulent flow properties for channels of this geometry. Keller and Rodi (1988) developed a two-dimensional k-ε model for predicting these properties theoretically. Their results are in agreement with a number of experimental studies surveyed by them. Arnold, Pasche and Rouve (1985) and Wood and Liang (1989) have investigated the dispersion characteristics of such channels.

This paper introduces a new method for solving the three-dimensional turbulent diffusion equation in channels of irregular cross-section where a steady source of effluent is present.

2 THE MATHEMATICAL MODEL

The turbulent advection diffusion equation for a neutrally buoyant, conservative contaminant can be simplified to equation (1) if the following assumptions are made:

1. The turbulent diffusivity tensor ε_{ij} is diagonal, with components ε_x, ε_y, ε_z,
2. no currents exist within the channel cross-section,
3. the dispersing plume is long and thin and hence the longitudinal turbulent diffusion can be neglected.

$$u\frac{\partial c}{\partial x} = \frac{\partial}{\partial y}\left(\varepsilon_y \frac{\partial c}{\partial y}\right) + \frac{\partial}{\partial z}\left(\varepsilon_z \frac{\partial c}{\partial z}\right) \qquad (1)$$

Here x is the downstream coordinate, and y and z the vertical and lateral coordinates respectively. U is the x velocity component and c is the contaminant concentration.

The boundary conditions on the cross-section boundaries are that there is no flux of material. At the cross-section denoted by x = 0, a source concentration distribution must be specified. Thus

$$c(0,y,z) = c_s(y,z) \qquad (2)$$

For convenience equation (1) is non-dimensionalised through the introduction of the following non-dimensional variables

$$x' = \frac{x}{d}, \quad y' = \frac{y}{d}, \quad z' = \frac{z}{d} \qquad (3)$$

$$u = \bar{u}\,\chi(y,z), \qquad (4)$$

$$\varepsilon_y = u_* d\,\psi_y(y,z), \quad \varepsilon_z = u_* d\,\psi_z(y,z) \qquad (5)$$

where $\bar{u}$ is the cross-sectionally averaged velocity, u_* is a shear velocity, and d is a representative lengthscale. χ, ψ_y and ψ_z are non-dimensional velocity and diffusivities respectively.

The choices for u_* and d are not unique in an irregular channel. We will take d to be the greatest flow depth in the channel and u_* to be $\sqrt{gdS}$ where S is the slope of the channel and g is gravity.

The concentration can be non-dimensionalised by the fully-mixed concentration, c_∞. So

$$c' = c/c_\infty \qquad (6)$$

where c_∞ is defined by

$$c_\infty = \int_A c_s \chi \, dA \qquad (7)$$

where A is the cross-sectional area. Thus equation 1 reduces to

$$\sqrt{\frac{8}{f}}\,\chi\frac{\partial c}{\partial x} = \frac{\partial}{\partial y}\left(\psi_y \frac{\partial c}{\partial y}\right) + \frac{\partial}{\partial z}\left(\psi_z \frac{\partial c}{\partial z}\right) \qquad (8)$$

where $f = 8u_*^2/\bar{u}^2$, is the friction factor, and the primes have been dropped.

3 SOLUTION METHOD

As the flow is assumed to be uniform downstream a separated solution of the form

$$c(x,y,z) = X(x)H(y,z) \qquad (10)$$

can be sought. This reduces equation (8) to the two-dimensional eigenfunction problem stated in equations (11) and (12).

$$\frac{\partial}{\partial y}\left(\psi_y \frac{\partial H}{\partial y}\right) + \frac{\partial}{\partial z}\left(\psi_z \frac{\partial H}{\partial z}\right) + \lambda\chi H = 0 \qquad (11)$$

with $\psi_{ij}\frac{\partial H}{\partial x_j}n_i = 0$ on Γ. (12)

Equation (12) is simply a statement of the no flux boundary conditions, **n** being a unit normal vector on the boundary Γ. Here λ is the eigenvalue corresponding to the eigenfunction H, and the general solution to the problem becomes

$$c(x,y,z) = \sum_{n=0}^{\infty} a_n \exp(-\sqrt{\frac{f}{8}}\lambda_n x)\, H_n(y,z) \quad (13)$$

The coefficients, a_n, can be found in the usual way from the source condition. Thus

$$a_n = \frac{\int_A c_s \chi\, H_n\, dA}{\int_A \chi\, H_n^2\, dA} \quad (14)$$

The eigenvalues and eigenfunctions of equations (11) and (12) possess many of the properties characteristic of their one-dimensional counterparts in standard Sturm-Liouville theory.

The eigenfunctions and eigenvalues can be calculated numerically. The flow domain is covered by a rectangular mesh of nodes (see figure 1) and a central finite-difference approximation to equation (11) is applied at each node. By assuming that all flow boundaries are vertical or horizontal, and ensuring that the boundaries lie midway between rows or columns of nodes, the zero-flux boundary conditions (which is taken to be zero concentration gradient) are simply approximated with a central difference.

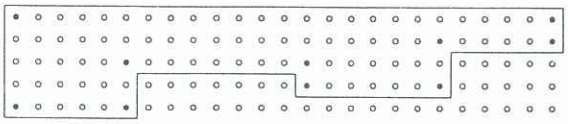

Figure 1. The channel cross-section is indicated by the solid lines. The nodes in the finite difference mesh are designated by the circles. The solid circles have no special significance.

If the nodes are labelled with the indices i and j, i referring to the row and j referring to the column, then equation (11) for an internal node, under the fintie difference approximation, reduces to a set of linear equations which take the form

$$a_{ij}H_{i-1j} + b_{ij}H_{i+1j} + c_{ij}H_{ij} + d_{ij}H_{ij-1} + e_{ij}H_{ij+1} = -\lambda f_{ij}H_{ij} \quad (15)$$

where

$$a_{ij} = \frac{1}{\Delta z^2}\psi_{z\ i-0.5\ j}, \quad b_{ij} = \frac{1}{\Delta z^2}\psi_{z\ i+0.5\ j} \quad (16)$$

$$c_{ij} = -\frac{1}{\Delta z^2}\left(\psi_{z\ i+0.5\ j} + \psi_{z\ i-0.5\ j}\right) - \frac{1}{\Delta y^2}\left(\psi_{y\ i\ j+0.5} + \psi_{y\ i\ j-0.5}\right) \quad (17)$$

$$d_{ij} = \frac{1}{\Delta y^2}\psi_{y\ i\ j-0.5}, \quad e_{ij} = \frac{1}{\Delta y^2}\psi_{y\ i\ j+0.5} \quad (18)$$

$$f_{ij} = \chi_{ij} \quad (19)$$

The indices j + 0.5 etc refer to locations in the mesh halfway between nodes, and Δy and Δz are the node spacings in the vertical and horizontal.

If node i,j has a neighbour which lies outside the channel boundaries then the boundary condition can be used to replace the external nodal value with that at node i, j. Thus equation (15) can be constructed at every node inside the channel cross-section. The resulting set of equations can be written as

$$\mathbf{Ah} = -\lambda\,\mathbf{Bh} \quad (20)$$

where A and B are NxN matrices, N being the number of internal nodes, and **h** is the eigenvector containing the unknown nodal values.

Standard numerical techniques, which take advantage of the symmetry of A and B, can be used to calculate the eigenvalues and eigenvectors of equation (20).

4 RESULTS

4.1 Velocity and Diffusivity Distributions

At this point no assumptions have been made regarding the form of the velocity or diffusivity distributions. The model allows these distributions to be specified as continuous fields or in a pointwise fashion. A number of different velocity and diffusivity models, based on rather simplistic assumptions, will be considered here.

If it is assumed that the flow is in local equilibrium and that lateral gradients in the flow are small the local shear stress at the bed must balance the driving gravitational force. Thus a local shear velocity can be defined as

$$u^*_{local} = \sqrt{g d_{local} S} \quad (21)$$

where the local depth has been used in equation (21). By taking the assumption of local equilibrium further we suggest that the lateral and vertical diffusivities should scale with the local depth. Thus in regions of the flow where the depth is less than maximum the diffusivities will be smaller that those in the deepest part of the channel by a factor of $\sqrt{\frac{d_{local}}{d_{max}}}$.

In addition the mean flow velocity will be expected to vary between regions of differing flow depth. The suggestion of Smith (1982), that the mean velocity should scale in the same fashion as the shear velocity, was supported by the experimental results of Nokes (1986) in a triangular channel. The experimental studies examined by Keller and Rodi (1988) also lend moderate support for such a relationship. This result has the nice consequence that the friction factor becomes an invariant of the channel, independent of local conditions.

Finally, near an abrupt change in channel depth it would be expected that the local horizontal shear would enhance the local turbulent intensities, thus increasing the turbulent diffusivities. This argument is supported by the numerical results of Keller and Rodi (1988). In the fourth model presented below this increase will be accounted for empirically by assuming that both diffusivities take on twice their normal values within one half depth of a change in channel depth.

The four velocity/diffusivity models used are as follows:

1. Uniform:

$$\chi = 1, \quad \psi_y = \frac{\kappa}{6}, \quad \psi_z = \frac{\kappa}{3}$$

where κ is von Karman's constant, generally taken to be 0.4. This is the most simple model where all quantities are assumed to be constant throughout the flow. The depth-averaged values relevant to a rectangular, laboratory channel (see Nokes, 1986) are used.

2. Uniform scaled:

$$\chi = \chi_0\left(\frac{d_{local}}{d_{max}}\right)^{0.5}, \quad \psi_y = \frac{\kappa}{6}\left(\frac{d_{local}}{d_{max}}\right)^{1.5}, \quad \psi_z = \frac{\kappa}{3}\left(\frac{d_{local}}{d_{max}}\right)^{1.5}$$

Variations with the vertical coordinate are neglected in this model but the scaling with local depth, discussed above, is now employed. The constant χ_0 is chosen to ensure that the cross-sectional average of χ is 1.

3. Non-uniform scaled:

The variations with the vertical coordinate are now incorporated into the distributions. The velocity will be assumed to have a power law dependence, the exponent of which is determined by a least squares best fit to a logarithmic profile. The vertical diffusivity has the commonly accepted parabolic shape and the horizontal diffusivity, after Nokes and Wood (1988), is assumed to have the same vertical dependence as the velocity. So

$$\chi = \chi_0(1+\alpha)y'^{\alpha}\left(\frac{d_{local}}{d_{max}}\right)^{1.5},$$

$$\psi_y = \kappa\, y'(1 - y')\left(\frac{d_{local}}{d_{max}}\right)^{1.5},$$

$$\psi_z = \frac{\kappa}{3}(1+\alpha)y'^{\alpha}\left(\frac{d_{local}}{d_{max}}\right)^{1.5}$$

The variable y' is a local vertical variable, being 0 at the bed and 1 at the free surface.

4. Empirical scaled:

The distributions are the same as in model 3 except the increased turbulent intensity near an abrupt change in channel depth is accounted for empirically, as discussed above.

4.2 First Eigenvalue and Eigenfunction

The first non-zero (smallest) eigenvalue and its corresponding eigenfunction play a fundamental role in the prediction of effluent dispersion in a channel. This mode is the last to decay in equation (13) and hence it determines the distance downstream of the source at which mixing is essentially complete. This smallest eigenvalue determines the mixing distance.

If the source is located in a position where the first eigenfunction vanishes then the coefficent for this mode a_1 is zero. In this case the second mode dominates downstream and the pollutant becomes fully mixed most rapidly. Such a source is referred to as the 'ideal source'.

It is the ability of this solution method to predict easily the form of the first eigenfunction and the value of the first eigenvalue which makes this semi-analytic solution method superior to a full numerical scheme.

Figure 2 presents contour plots of the first eigenfunction for each of the four velocity/diffusivity models. The channel cross-section has been chosen arbitrarily. Also indicated on each of the diagrams is the value of the first eigenvalue.

Model 1 can be seen to predict a rather larger eigenvalue than the other three model,s indicating a 60% shorter mixing distance. This is due to the fact that model 1 does not account for the decrease in diffusivities in the shallow portions of the channel. The other three models show little variation, although model 4 with its increased mixing capabilities near steps in the channel bed predicts a slightly shorter mixing distance. For channels with significant variations in flow depth the simplistic model 1 would seem to be inappropriate.

The zero contour of the first eigenfunction for models 2, 3 and 4 are nearly coincident while that for model 1 lies rather closer to the centre of the channel. This variation will become more important as the depth variations in the channel increase.

4.3 A Comparison With Wood and Liang (1989)

Wood and Liang(1989) measured point concentrations downstream of a steady source in a main channel/flood plain geometry. Their two-dimensional solution showed

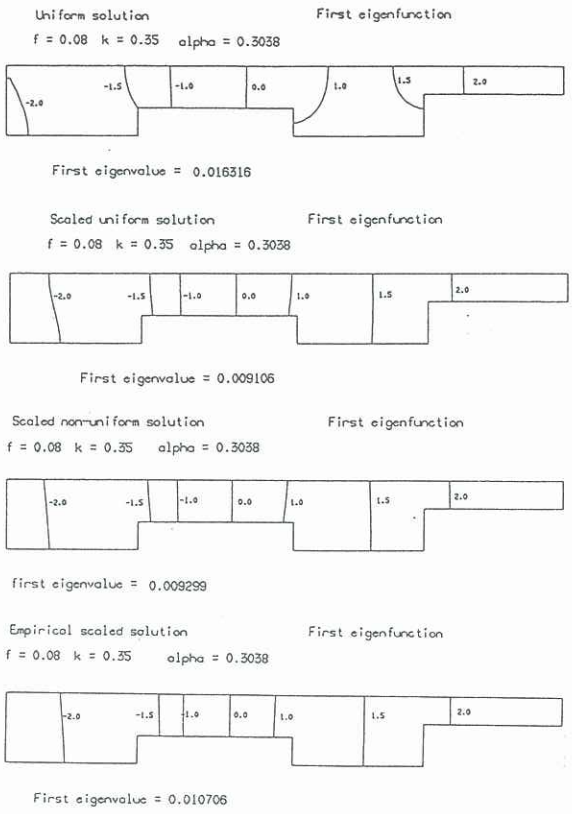

Figure 2: Plots of the first eigenfunction in a channel with an arbitrarily chosen cross-section for each of the velocity/diffusivity models. The labelled curves are eigenfunction contours. The eigenvalues are also given in each plot.

qualitative agreement with their experimental results. As their measurements were all made within the near-source region (i.e. where vertical and lateral concentration gradients are present) the present model will be able to produce more detailed predictions of the concentration distribution.

Figures 3 and 4 present the predictions of models 1 and 4 respectively as a set of concentration contour plots at a number of downstream sections for one of their experiments. Figure 5 reproduces the actual measurements of Wood and Liang. In this particular experiment the source was placed in the main channel near the step.

The predictions of the two models differ in a number of ways. Model 1 predicts that the effluent is mixed more rapidly into and across the flood plain than does model 4 but the experimental results are not capable of differentiating between the two models. However the movement of the maximum concentration in the plume is more acurately predicted by model 4. The experimental results demonstrate that at the first section downstream of the source (x = 19.6) the maximum in the plume has dropped to the bed and the maximum concentration in the plume is a little more than 5. Both the movement and magnitude of the maximum are well predicted by model 4. On the other hand the uniform model does not predict the downward movement of the maximum until x = 49. The measured decrease, with distance downtream, of the maximum concentration in the flow is also more acurately modelled by the more sophisticated model.

It would seem that the incorporation of the velocity and turbulent diffusivity dependence on local depth, in some form, is necessary for accurate predictions of the turbulent mixing in channels with a complex cross-section.

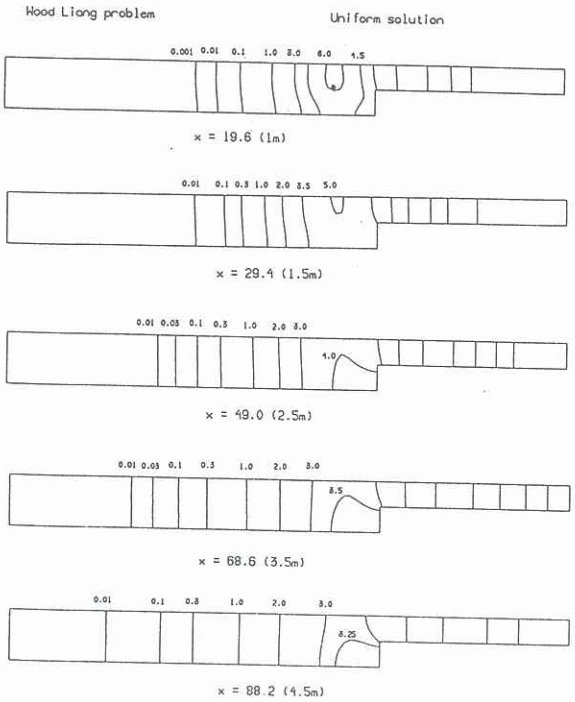

Figure 3: Concentration predictions, using model 1, of the Wood and Liang (1988) flow. The source location is marked by an asterisk in the first plot. The labelled curves are concentration contours.

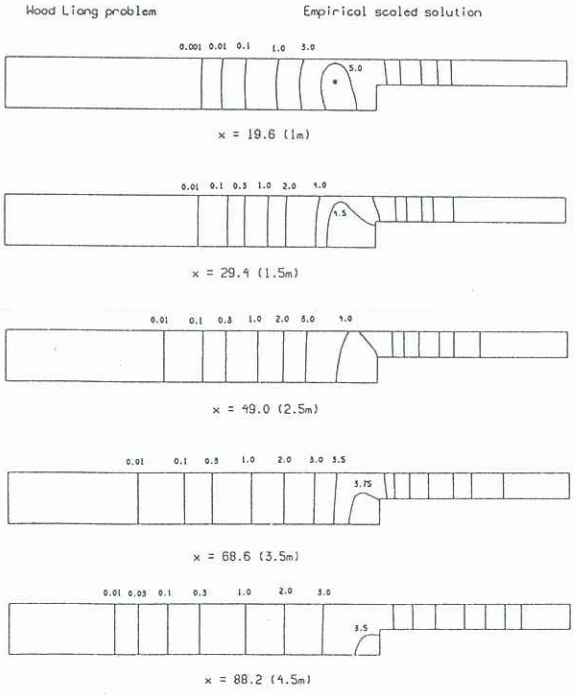

Figure 4: Concentration predictions, using model 4, of the Wood and Liang (1988) flow. The source location is marked in the first plot. The labelled curves are concentration contours.

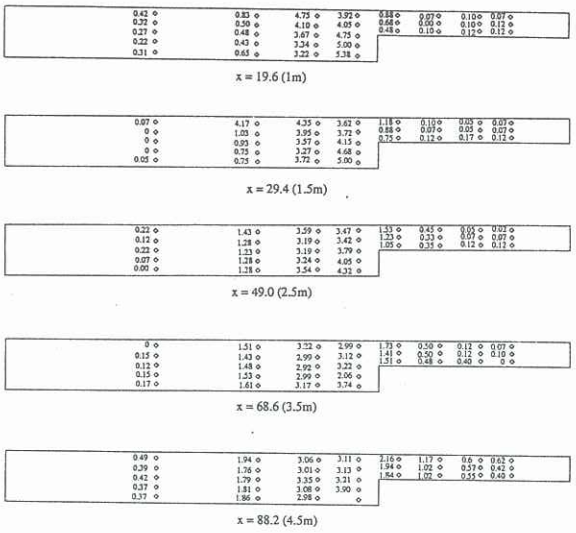

Figure 5: The concentration measurements of Wood and Liang (1988) reproduced from their paper. These results are for the same flow conditions as figures 3 and 4.

5 CONCLUSIONS

A new numerical procedure for predicting three-dimensional turbulent dispersion in uniform channels of any cross-sectional shape has been presented. In the near-source mixing zone where both vertical and lateral mixing are important in the dilution of the pollutant a three-dimensional solution offers more detailed information about the concentration field than a two-dimensional solution. Comparison with experiment implies that a mathematical model must incorporate the dependence on local depth of velocity and turbulent diffusivities if the mixing in a compound channel is to be accurately predicted.

REFERENCES

ARNOLD U., PASCHE E., ROUVE G. (1985) Mixing in rivers with compound cross-section. IAHR 21st Congress Proceedings, Melbourne, 2, pp 167-172.

KELLER R. J., RODI W. (1988) Prediction of flow characteristics in main channel/flood plain flows. Journal of Hydarulic Research, 26, No. 4, pp425-441.

NOKES R. I. (1986) Problems in turbulent dispersion. Ph.D. Thesis, Dept. of Civil Engineering, University of Canterbury, New Zealand (also Civil Engineering Research Report, No. 86/8)

NOKES R. I., WOOD I. R. (1988) Vertical and lateral turbulent dispersion: some experimental results. Journal of Fluid Mechanics, 187, pp 373-394.

SHIONO K., KNIGHT D. W. (1991) Turblent open-channel flows with variable depth across the channel. Journal of Fluid Mechanics, 222, pp 617-646.

SMITH R. (1982) Where to put a steady discharge in a river. Journal of Fluid Mechanics, 115, pp 1-11.

WOOD I.R., LIANG TONG (1989) Dispersion in an open channel with a step in the cross-section. Journal of Hydraulic Reseach, 27, No. 5, pp 587-601.